Bone Reports 12 (2020) 100266

Contents lists available at ScienceDirect

Bone Reports

journal homepage: www.elsevier.com/locate/bonr

Age-related and sex-specific effects on architectural properties and biomechanical response of the C57BL/6N mouse femur, tibia and ulna

Hammad Mumtaz[a], Mark Dallas[b], Mark Begonia[c], Nuria Lara-Castillo[b], JoAnna M. Scott[d], Mark L. Johnson[b], Thiagarajan Ganesh[a,*]

[a] University of Missouri-Kansas City, Department of Civil and Mechanical Engineering, 350K Robert H. Flarsheim Hall, 5110 Rockhill Road, Kansas City, MO 64110, USA
[b] University of Missouri-Kansas City, School of Dentistry, Department of Oral and Craniofacial Sciences, Room 3143, 650 E 25th Street, Kansas City, MO 64108, USA
[c] Virginia Polytechnic Institute and State University, Biomedical Engineering and Mechanics, 343 Kelly Hall, 325 Stanger Street MC 0298, Blacksburg, VA 24061, USA
[d] University of Missouri-Kansas City, Office of Research and Graduate Programs, Kansas City, MO 64108, USA

ARTICLE INFO

Keywords:
Aging
Gender
C57BL/6N
Three-point bending
Femur
Tibia
Ulna
Biomechanical parameters

ABSTRACT

Aging is known to reduce bone quality and bone strength. We sought to determine how aging affects the biomechanical and architectural properties of various long bones, and if sex influences age related differences/changes. While researchers have extensively studied these changes in individual bones of mice, there is no comprehensive study of the changes in the bones from the same mice to study the changes with aging. We performed three point bending tests and microcomputed tomography (microCT) analysis on femurs, tibiae and ulnae. Three point bending tests were utilized to calculate biomechanical parameters and imaging was also performed using high resolution microCT to reveal both cortical and trabecular microarchitecture C57BL/6N mice were divided into three age groups: 6, 12 and 22 months. Each age and sex group consisted of 6–7 mice. The ultimate load to failure (UL), elastic stiffness (ES), modulus of elasticity (E) and the moment of inertia about bending axis (MOI) for each bone was calculated using three point bending test. MicroCT scans of all the bones were analyzed to determine cortical bone volume per tissue volume (C.BV/TV), trabecular bone volume per tissue volume (Tb.BV/TV), cortical bone area (B.Ar) using CTAn's microCT analysis and tested for correlation with the biomechanical parameters. Mean (standard error) values of UL in femur decreased from 19.8(0.6) N to 12.8(1.1) N ($p < .01$) and 17.9(0.6) N to 14.6(1.0) N ($p = .02$) from 6 to 22 months groups in males and females respectively. Similarly, UL in tibia decreased from 19.8(0.5) N to 14.3(0.2) N ($p < .01$) and 14.4(0.6) N to 9.5(1.0) N ($p < .01$) from 6 to 22 months group in males and females respectively. ES in femur decreased from 113.2(7) N/mm to 69.6(6.7) N/mm ($p < .01$) from 6 to 22 months in males only. ES in tibia decreased from 78.6(3.2) N/mm to 65.0(2.3) N/mm ($p = .01$) and 53.1(2.9) N/mm to 44.0(1.7) N/mm ($p = .02$) from 6 to 22 months in males and females respectively. Interestingly, ES in ulna increased from 8.2(0.8) N/mm to 10.9(1.0) N/mm ($p = .051$) from 6 to 22 months of age in females only. E in femur decreased from 4.0(0.4) GPa to 2.8(0.2) GPa ($p = .01$) and 6.7(0.5) GPa to 4.5(0.4) GPa ($p = .01$) from 6 to 22 months of age in males and females respectively while tibia showed no change. However, E in ulna increased from 7.0(0.8) GPa to 11.0(1.1) GPa ($p = .01$) from 6 to 22 months of age in females only. Changes in age and sex-related bone properties were more pronounced in the femur and tibia, while the ulna showed fewer overall differences. Most of the changes were observed in biomechanical compared to architectural properties and female bones are more severely affected by aging. In conclusion, our data demonstrate that care must be taken to describe bone site and sex-specific, rather than making broad generalizations when describing age-related changes on the biomechanical and architectural properties of the skeleton.

1. Introduction

Normal human aging after the 4th–5th decade of life is associated with decline in bone mass and mechanical properties (Boskey and Coleman, 2010). This age related bone loss is a major cause of osteoporotic fractures in both men and women (Ensrud et al., 1995; Melton III, 1997; Glynn et al., 1995). Hip, spine and wrist are the most common sites of fracture but the worst outcomes are associated with the hip

* Corresponding author at: University of Missouri-Kansas City, 350K Robert H. Flarsheim Hall, 5110 Rockhill Road, Kansas City, MO 64110, USA.
E-mail address: ganesht@umkc.edu (T. Ganesh).

https://doi.org/10.1016/j.bonr.2020.100266
Received 19 September 2019; Received in revised form 30 March 2020; Accepted 2 April 2020
Available online 23 April 2020

fracture (Harvey et al., 2010). In United States alone, approximately, more than > 2 million incidences of fracture were reported in 2005 which costs $17 billion. 71% of all the fractures were reported in women and 75.5% of all the cost related to these fractures were associated with women (Begun, 2015). This age-related bone loss that leads to increased risk of fracture and increased impact on economy is now a major focus of modern day research to reduce its consequences.

In humans, dual energy X-ray absorptiometry (DXA) is commonly used to measure bone mineral density (BMD), which is considered the "gold" standard for monitoring bone loss and predicting risk of bone fracture. However, with DXA alone, it is difficult to get a clear and comprehensive understanding of the causes of fragility fractures and hence there is a need to investigate how the function of the bone changes with age (Begun, 2015). A study on postmenopausal women showed that the mechanical heterogeneity of the bone tissue determines the quality of bone (Vennin et al., 2017).

To investigate changes in microarchitecture, collagen structure and mineral composition, and influences of biochemical cues on aging, mouse models have been commonly used in various studies (Boskey and Imbert, 2017; Jilka, 2013; Syed and Hoey, 2010; Ferguson et al., 2003). A significant portion of bone mass and mechanical properties is dependent on the strain of mice used. Studies with different inbred mouse strains demonstrated large differences in bone density, mechanical properties and have confirmed the influence of multiple genes contributing to these differences. Beamer et al. identified specific genes that results in the changes in specific properties of bone in different inbred mouse strains (Beamer et al., 1996). Genome wide association studies (GWAS) have also identified several loci involved in regulating osteoblast activity and bone mass (Mesner et al., 2019). The three-point bending test is commonly used in the evaluation of bone strength (Jämsä et al., 1998). Brodt et al. suggested that the changes in structural rigidity and ultimate load is dependent more on the increase in the material properties compared to the increase in cross sectional geometry (Brodt et al., 1999). Age associated bone loss in mice may result from both osteoblast insufficiency and enhanced resorption. Ferguson et al. showed that male C57BL/6J is a suitable mice for aging related studies and observed that while the whole bone elastic stiffness, energy to fracture, cortical thickness and percent mineralization decreased at 104 weeks of age from their peak values, the periosteal perimeter and cross sectional moment of inertia increased to compensate for some of the biomechanical property losses in male femurs and humeri (Ferguson et al., 2003). A study by Sommerville et al. on C57BL/6 mice tibia showed that most of the microCT parameters i.e. bone mineral density (BMD) and cross-sectional moment of inertia tend to increase with growth and then level off some time before 6 months of age (Somerville et al., 2004). However, this study was limited to mice under the age of 12 months.

While the literature contains numerous studies examining the material, architectural and mechanical properties of different bones in the mouse skeleton, only a few studies have performed a systematic analysis of different bones in the same mouse. Schriefer et al. examined the mechanical properties of the mouse tibia, femur, humerus, third metatarsal and radius for both C57BL/6 and the high bone mass C3H/HeJ mice. They found significant differences in mechanical properties of the different bones and different strains. Using computational models they noted that significant measurement error was inherent in three point bending tests depending upon the bone. Bones with the highest span to mid-shaft diameter ratio such as the radius were better for testing as they lower measurement errors and variability (Schriefer et al., 2005). Glatt et al. used peripheral DXA, microCT and histomorphometry to examine changes in total body bone mineral density (BMD) and trabecular bone volume (in L5 vertebrae and the femur) and showed that age related deterioration in trabecular architecture differed between the sexes and was more pronounced in females (Glatt et al., 2007).

Heveran et al. studied the effect of chronic kidney disease (CKD) and aging (3, 18 and 21 month old) C57BL/6 mice femur and tibia and found that aging and CKD has different effects on bone properties. Whole bone strength, elastic modulus, nanoindentation modulus decreased with aging while CKD resulted in decreased work to fracture and variation in tissue bone tissue modulus and composition and increased collagen strain (Heveran et al., 2019).

While researchers have extensively studied the changes in the architecture and biomechanical properties with aging of individual bones of mice such as the femur, tibia and ulna, there is no comprehensive study of the changes in the bones from the same mice. All three bones are considered here since the ulna and tibia are frequently used in most in vivo studies and the femur is studied as it has a relatively uniform cross-section and is suitable for comparative studies. Hence, in this paper, we studied the biomechanical response by three point bending and architectural properties by microCT of the ulna, femur and tibia from the same animal in male and female C57BL/6N mice at 6, 12 and 22 months of age. Our data demonstrate bone site-specific changes occurring in the skeleton during aging in terms of biomechanical and architectural properties. Importantly, these findings suggest caution when measuring a single bone site and generalizing those findings to the rest of the skeleton.

2. Materials and methods

2.1. Specimen preparation

C57BL/6N mice obtained from the NIH Mouse Aging Colony at Charles Rivers Laboratories were divided into three age groups: 6, 12 and 22 months. There were six males (weight 35.1 ± 2.4 g) and six females (weight 24.3 ± 1.5 g) in the 6-month group, six males (weight 37.4 ± 2.1 g) and six females (weight 27.9 ± 1.5 g) in the 12-month group and seven males (weight 34.1 ± 3.8 g) and seven females (weight 30.3 ± 4.5 g) in the 22-month group. The number of mice was chosen based on statistical analyses conducted in a previous study (Lara-Castillo et al., 2015). The UMKC IACUC approved all animal studies.

The mice were euthanized by CO_2 inhalation followed by cervical dislocation. Skin was removed from hind limbs and forearms and the soft tissues were removed from the left ulnae, right tibiae, left femurs and then wrapped in a PBS soaked gauze. The bones were stored in the −20 °C freezer until needed.

2.2. Biomechanical parameters

2.2.1. Three-point bending test

All three types of bones were subjected to the three point bending test using BOSE 3230 biomechanical tester with a maximum load capacity of 450 N (Jepsen, 2009). The samples were thawed for ~30 min before testing. Any residual soft tissues, muscles and ligaments were carefully removed from each bone sample using tweezers and scissors. However, for tibia testing, the fibula was excised in order to create a large enough gap for the loading cap to pass through (~8 mm). Prior to testing the length, minimum and maximum diameter and weight was measured for each sample. The left and right overhangs were measured after the sample was placed on the BOSE machine fixture.

A span length of 7.6 mm was used for femurs and ulnae while 10 mm was used for tibiae. Femurs were positioned by keeping the anterior – posterior axis in the loading direction and medial - lateral axis in the bending direction. Ulnae were placed with the lateral - medial axis in the loading direction and the cranial - caudal axis in the bending direction. Tibiae were tested while keeping the posterior - anterior axis in the loading direction and the lateral - medial axis in the bending direction. The femur, ulna and tibia loaded are shown in Fig. 1. All the bones were centered on the supports and the force was applied vertically to the midshaft at a constant speed of 0.155 mm/s until it fractured.

Fig. 1. Femur (left), Tibia (middle) and Ulna (right) loaded in three point bending test.

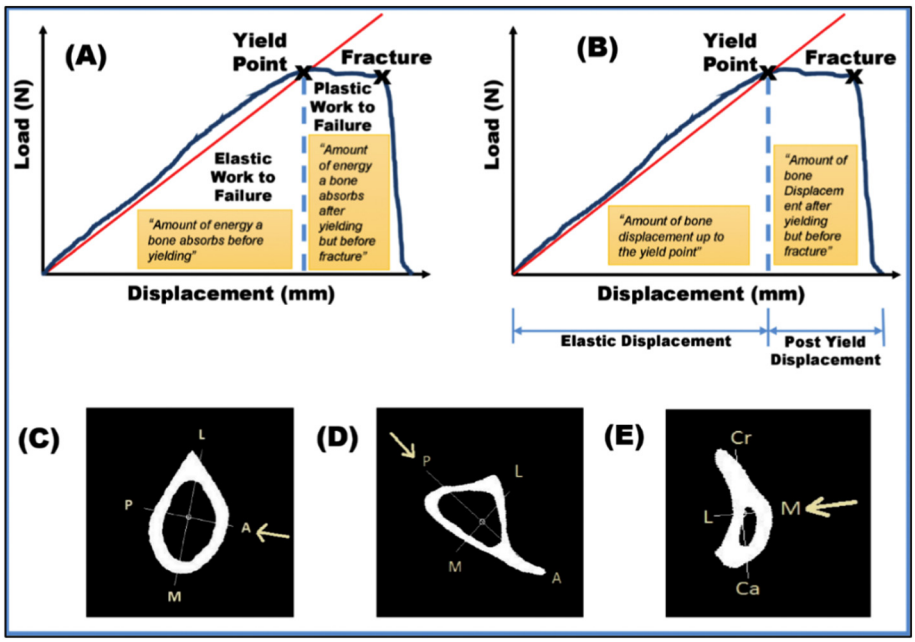

Fig. 2. Calculation of (A) elastic and plastic work to failure (B) displacement in elastic and plastic regions and cross section of (C) Femur, (D) Tibia & (E) Ulna showing actual loading orientation for the calculation of bending strength and moment of inertia using BoneJ.

2.2.2. Biomechanical parameters estimation

The biomechanical parameters were determined by three-point bending test on each bone sample. The statistical comparisons of all the calculated biomechanical parameters between the age groups were determined. Differences observed in 12 and 22 months in each parameter with reference to 6 months group are marked with an asterisk (*) on the graph. The biomechanical parameters calculated include Ultimate Load (UL), Elastic Stiffness (ES), Modulus of Elasticity (E), Moment of Inertia (MOI), Total Work to Failure (TWTF), Elastic Work to Failure (EWTF), Plastic Work to Failure (PWTF), Elastic Displacement (EDISP), Post Yield Displacement (PYD), Tensile Strength (TST) and Compressive Strength (CST) in both male and female groups.

2.2.3. Estimation of ultimate load & elastic stiffness

A load displacement curve was obtained from the three point bending test. From the curve, the ultimate load (UL) was calculated which is the maximum force that a bone experiences during the three point bending test. The elastic stiffness (ES) of the bone was estimated from the slope of the linear region of the curve.

2.2.4. Estimation of work to failure & displacement

Total work to failure (TWTF), which is the amount of energy a bone absorbs before breaking, was calculated from the area under the curve. The area under the curve was then divided into two regions by defining the yield point occurring at 95% change in secant stiffness. The two regions were named elastic region and plastic region, to determine the work to failure and displacements in those regions. The elastic work to failure (EWTF), which is defined as the amount of energy a bone absorbs before yielding, and the plastic work to failure (PWTF), which is defined as the energy a bone absorbs after yielding and before fracture were calculated (see Fig. 2).

Total displacement was calculated and divided into two parts i.e. elastic displacement (EDISP) which was defined as the amount of bone displacement up to the yield point and post yield displacement (PYD) which is defined as the amount of displacement after yielding but before fracture.

2.2.5. Moment of inertia

The moment of inertia (MOI) about the bending axis was calculated using ImageJ using the actual loading orientation. The images of orientation of each type of bone were captured using a microCT imaging system and then compared with the microCT images of the bone in literature to determine the loading and bending axis. The average moment of inertia of all the slices within the span was used to calculate moment of inertia. Every slice was 9.6 μm in thickness and hence we took 791 slices for femurs and ulnae (7.6 mm span) and 1042 slices for tibiae (10 mm span) to calculate the moment of inertia. The left and right overhangs were used to determine the starting and the ending slice.

2.2.6. Calculation of Young's modulus

Young's modulus (E) was calculated using Eq. (1).

$$E = \frac{(ES)l^3}{48I} \quad (1)$$

Where, ES is the elastic stiffness (N/mm), l is the span length (mm)

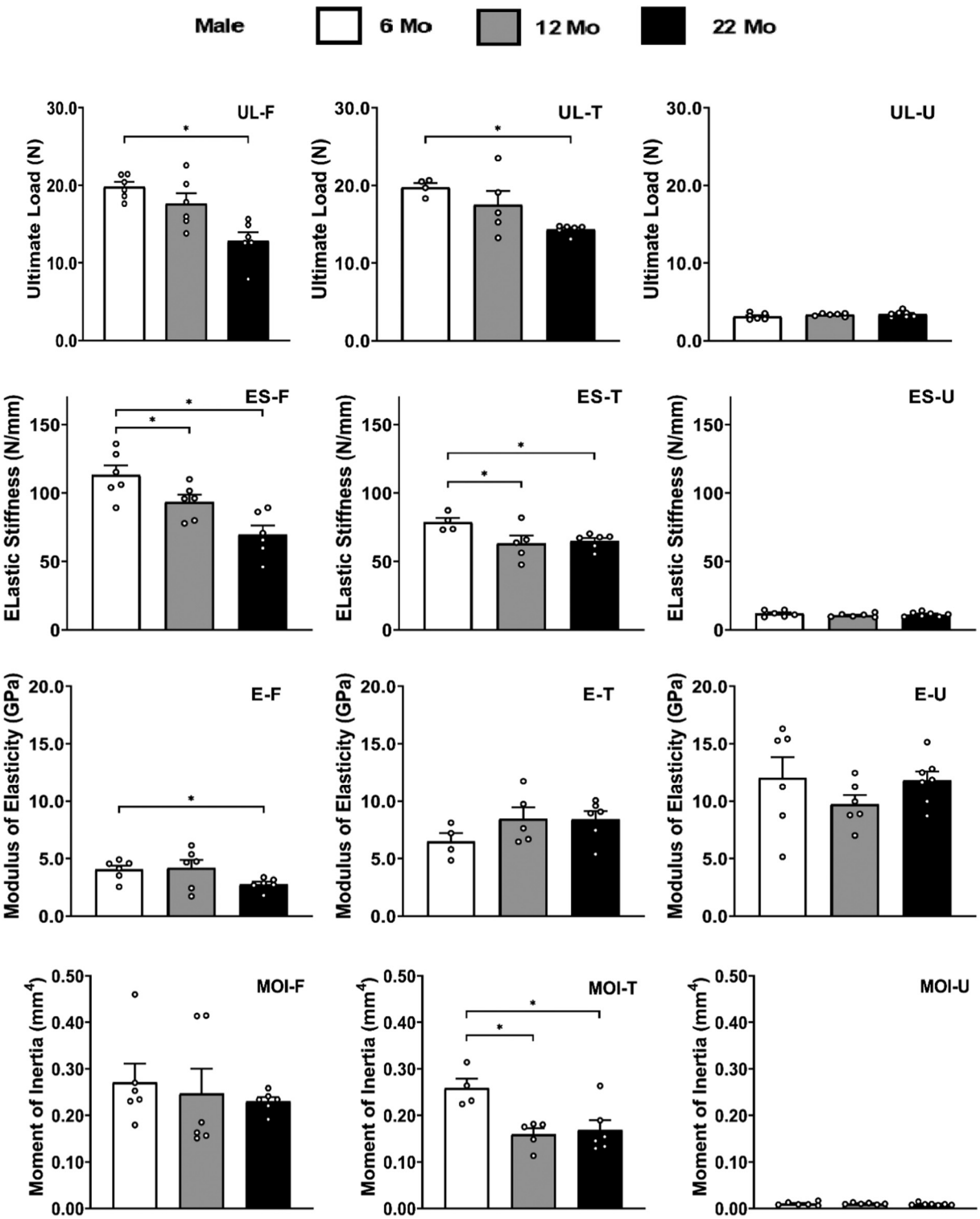

Fig. 3. Biomechanical parameters males: Ultimate load (UL), Elastic stiffness (ES), Modulus of elasticity (E), and Moment of inertia (MOI) in Femurs (F), Tibiae (T), and Ulnae (U). Values that are too close are staggered apart to help with differentiation. (Data are individual value and mean ± standard error).

and I is the average moment of inertia (mm^4).

2.2.7. Calculation of tensile strength

The tensile strength (TST) of the bone was calculated based on the geometry of the mid slice. The strength value is calculated assuming a flexural behavior. For mice bone tested using three point bending shear deformation is also likely to be influential. Since the failure is instantaneous and occurs when the tensile stress reaches the strength of the bone, it would be reasonable to state that the tensile stress is the tensile strength of the bone. However, the compressive stress (CST) is not the compressive strength and is the compressive stress when the tensile strength is reached. It is calculated here to compare it with the tensile strength.

The distance between the centroid and the periosteal points of the cross-section at the load location were determined using ImageJ. The strength values were calculated using Eq. (2). The distance from the

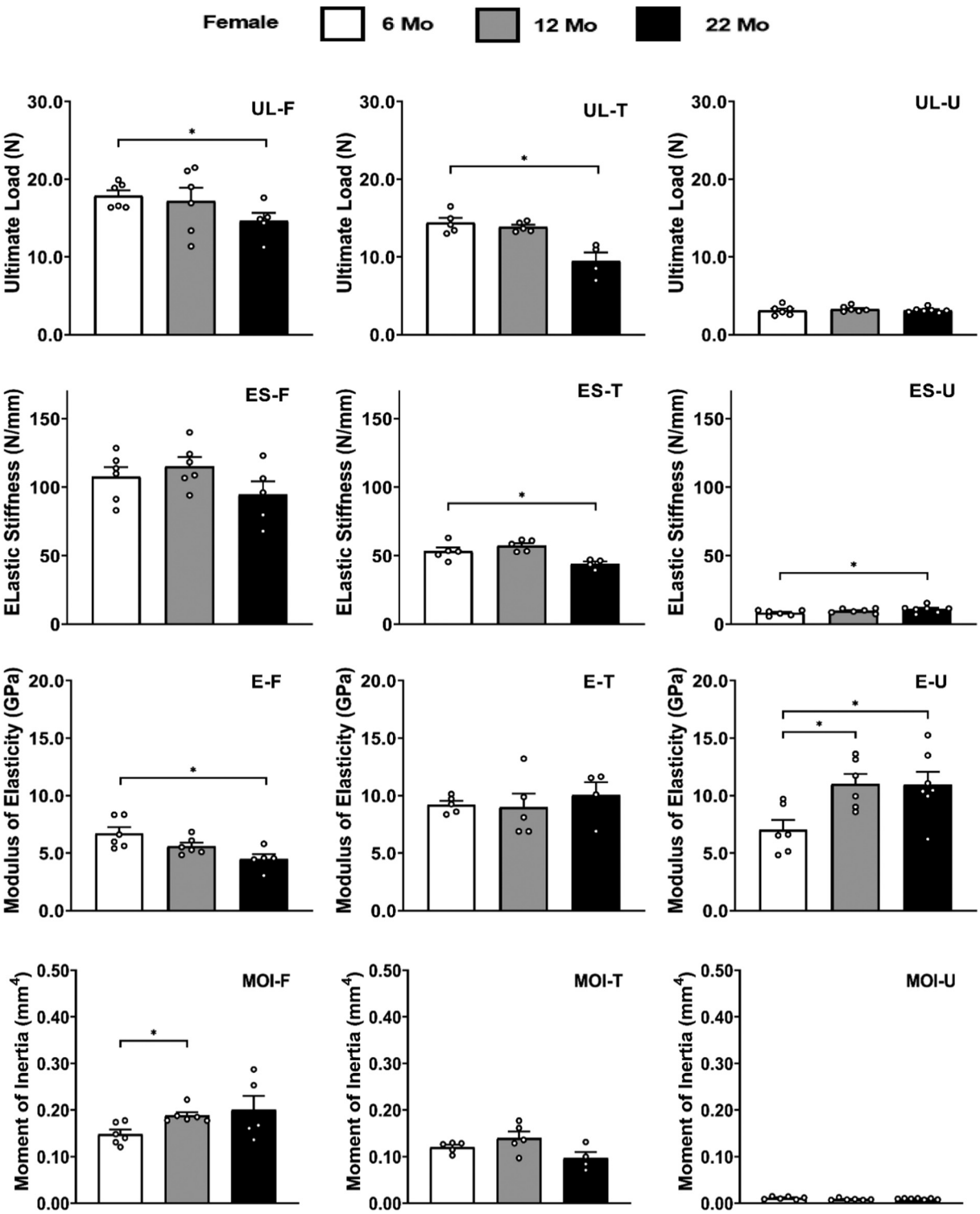

Fig. 4. Biomechanical parameters females: Ultimate load (UL), Elastic stiffness (ES), Modulus of elasticity (E), and Moment of inertia (MOI) in Femurs (F), Tibiae (T), and Ulnae (U). (Values that are too close are staggered apart to help with differentiation).

centroid point to the farthest point on the loading axis towards the loading surface gave us a compressive stress at failure while the distance from centroid to the farthest point away from the loading surface was used to calculate the tensile strength.

$$Bending\ Strength = \frac{Mc}{I} \quad (2)$$

where $M = Bending\ Moment = \frac{P_{max} l}{4}$ (N.mm), P_{max} *is the* Ultimate Load (N), l is the span length (mm), c is the distance (mm) from the centroid to the farthest point on the cross section, and I (mm^4) is the moment of inertia about bending axis. Bending strength was calculated in MPa units.

2.3. Statistical analysis

Linear regression with robust standard errors was used to test

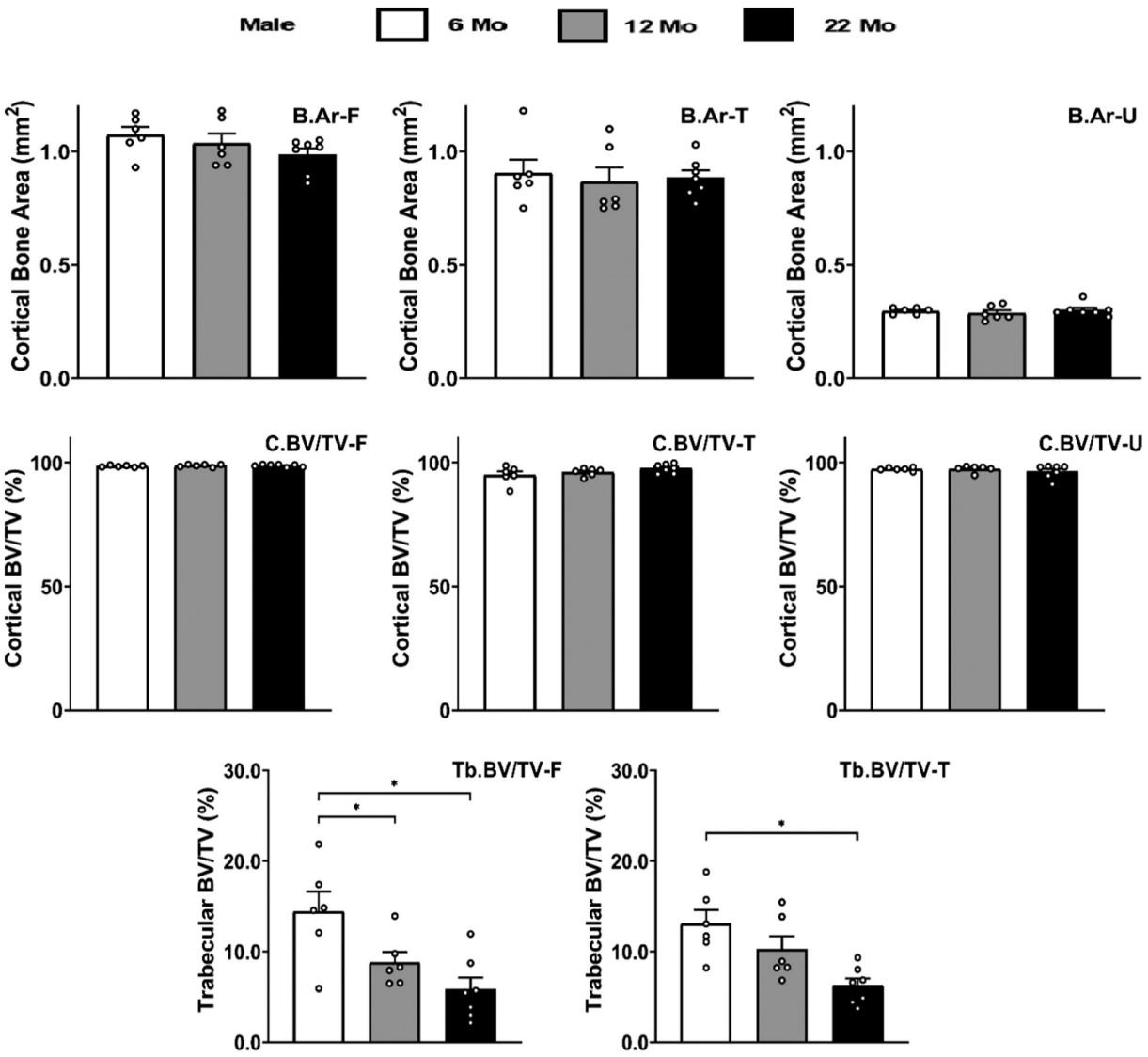

Fig. 5. MicroCT parameters males: Cortical bone area (B.Ar), Cortical BV/TV (C.BV/TV), and Trabecular BV/TV (Tb.BV/TV) in Femurs (F), Tibiae (T), and Ulnae (U). (Values that are too close are staggered apart to help with differentiation.)

associations between age and biomechanical parameters within gender and between age and microCT parameters within gender for each bone type. Linear regression was also used for all age group comparisons. Pearson correlation was utilized to evaluate all correlations of interest. All analysis was performed in Stata 15.1. The significance level was set to 0.05 a priori.

2.4. Micro-CT analysis

The mouse bones were scanned in the Bruker Skyscan 1174 at a nominal resolution of 9.6 μm employing an aluminum filter 0.5 mm thick and an applied x-ray tube voltage of 50 kV. Camera pixel binning was not applied. The scan orbit was 180/360 degrees with a rotation step of 0.4 degrees. Reconstruction was carried out with a modified Feldkamp algorithm using the SkyScanTM NRecon software accelerated by GPU3. Gaussian smoothing, ring artefact reduction and beam hardening correction were applied.

The stack of the reconstructed images was analyzed in CTAn software. Fifty slices from the mid diaphysis were selected for each type of bone to calculate the cortical bone parameters. The minimum threshold was set to 55 and maximum was set to 255 for all the bones. Hundred slices from distal femur and proximal tibiae were selected to calculate the trabecular bone parameters. The minimum threshold was set to 45 and maximum was set to 95 for both femur and tibiae. We used Bruker's CTAn software to calculate these parameters in which we are able to isolate the cortical and the trabecular bone regions using polygonal ROI tool. The software calculates the total volume based on our ROI and the respective bone volume within the selected ROI in either cortical or trabecula region. Trabecular bone analysis was not done on ulnae.

3. Results

3.1. Biomechanical parameters

3.1.1. Male femur, tibia & ulna

The effects of aging on the biomechanical parameters of male femurs, tibiae and ulnae are shown in Fig. 3. Ulnae parameters in large scale are also shown in supplementary Fig... S1. Ultimate load decreased significantly at 22 months of age compared to 6 months in both male femurs and tibiae but no change was observed in ulnae. Ultimate load in femurs was reduced by 35.28% and 27.59% in tibiae. Elastic stiffness decreased significantly at 12 and 22 months of age compared to 6 months in both femurs and tibiae while no change was observed in ulnae. Modulus of elasticity decreased only in femurs from 4.04 GPa at

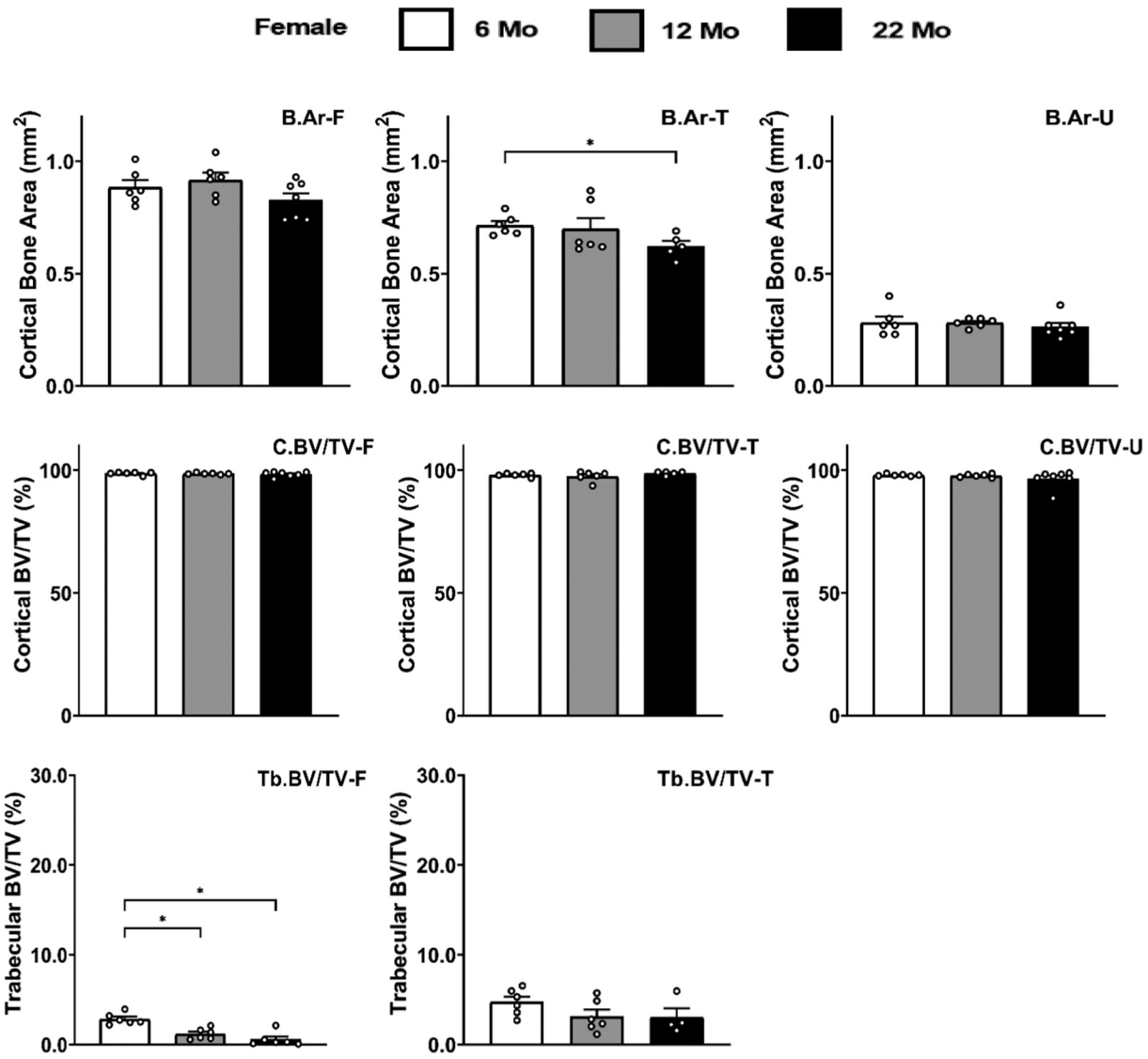

Fig. 6. MicroCT parameters females: Cortical bone area (B.Ar), Cortical BV/TV (C.BV/TV), and Trabecular BV/TV (Tb.BV/TV) in Femurs (F), Tibiae (T), and Ulnae (U). (Values that are too close are staggered apart to help with differentiation).

6 months to 2.77 GPA at 22 months of age and moment of inertia decreased in tibiae at 12 and 22 months of age.

3.1.2. Female femur, tibia & ulna

The effects of aging on the biomechanical parameters of female femurs, tibiae and ulnae are shown in Fig. 4. Ulnae parameters in large scale are also shown in supplementary Fig.. S2. Like males, ultimate load decreased significantly at the age of 22 months in both femur and tibiae while there was no change observed in ulnae. Ultimate load reduced by 18.18% in femurs while 34.10% in tibiae. Elastic stiffness decreased in tibiae from 53.15 N/mm to 44.06 N/mm and increased in ulnae from 8.23 N/mm to 10.87 N/mm at the age of 22 months. Modulus of elasticity decreased in femur at 22 months of age from 6.72 GPa to 4.48 GPa and increased from 7.03 GPa to 11.01 GPa at 12 and 10.97 GPa at 22 months of age in ulnae. Moment of inertia increased only in femurs at the age of 12 months.

3.2. Micro-CT analysis

3.2.1. Male femurs, tibiae and ulnae

The cortical BV/TV and the cortical bone area did not change in any of the bones. Trabecular BV/TV decreased significantly in femur at 12 and 22 months of age while it decreased significantly in tibia at the age of 22 months only. The effects of aging on the microCT parameters of male femurs, ulnae and tibiae are shown in Fig. 5.

3.2.2. Female femurs, tibiae and ulnae

Cortical BV/TV did not change in female bones while cortical bone area reduced in ulnae at the age of 22 months. Trabecular BV/TV reduced only in femur at 12 and 22 months of age. Trabecular BV/TV of male femurs were found to be 5, 7 and 10 times higher than the female femurs at 6, 12 and 22 months old groups respectively. Hence females appear to lose the trabecular bone in femurs earlier than the males during aging. The effects of aging on the microCT parameters of female femurs, ulnae and tibiae are shown in Fig. 6.

4. Discussions and conclusions

We hypothesized that both genders will display a significant decrease in biomechanical response at the age of 12 months and 22 months compared to 6 months in all the bones. While size and shape are the morphological traits that determine the strength of the bone (Jepsen, 2009), the composition and mechanical properties of the bones will vary as a function of age. Understanding the factors controlling the

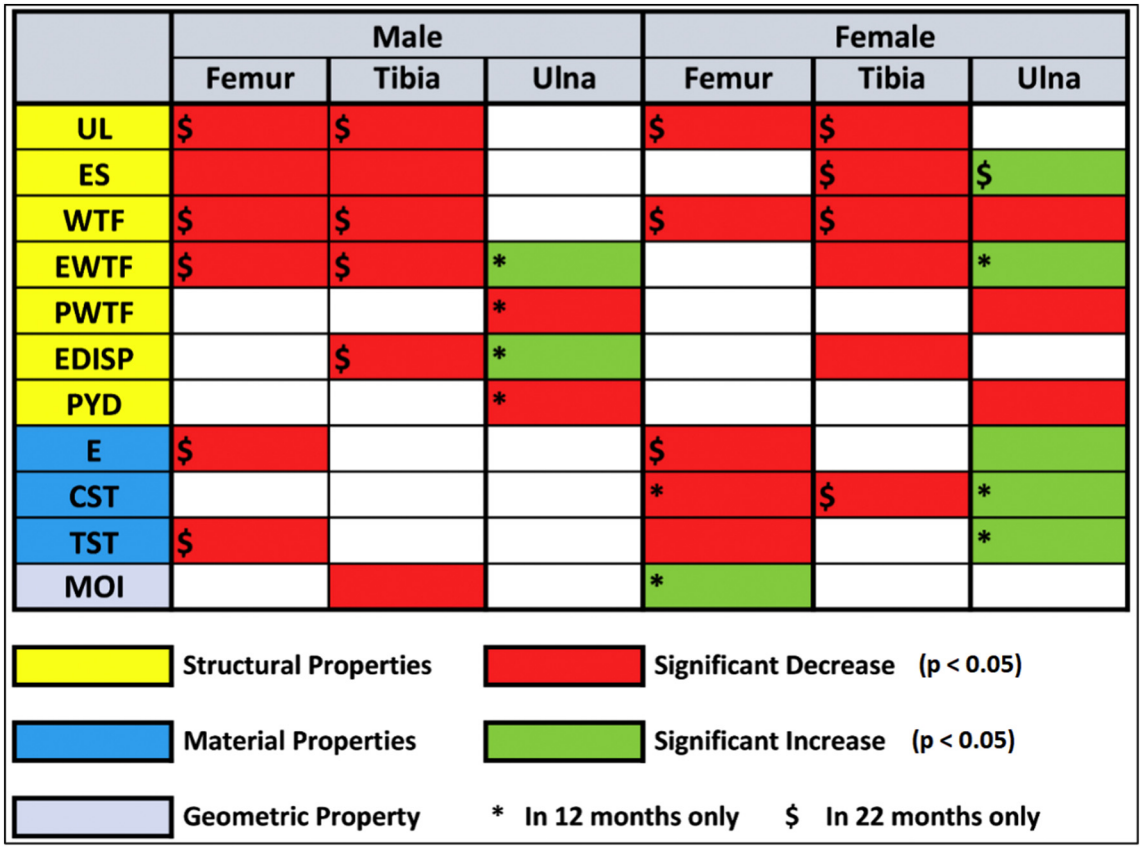

Fig. 7. Summary of biomechanical parameters grouped as structural, material and geometric properties (Both males and females) and the significant changes at 12 months & 22 months of age while *p* value was set to 0.05.

aging of cells and identifying specific pathways that control these factors at different ages is a great challenge (Boskey and Coleman, 2010).

In Fig. 7, the biomechanical response of all the bones is summarized and the changes observed are described. The biomechanical parameters are grouped into structural, material and geometric properties.

The summary of the parameters in Fig. 7, illustrates the age and sex effects on the biomechanical response of femurs, tibiae and ulnae. The red tab shows a significant decrease at 12 and 22 months of age compared to 6 months while the green tab shows a significant increase at 12 and 22 months compared to 6 months. An asterisk (*) was used to denote statistically significant changes only at 12 months while the dollar ($) sign demarks significant changes only at 22 months.

Ferguson et al. studied the age-related changes in male femur of C57BL/6 mice of age between 1 and 26 months and found a substantial increase in bone size, mineral mass and mechanical properties at the age of 3 months. Cross sectional moment of inertia at the mid diaphysis region of femur was increased throughout this study. However, Elastic 's modulus increased to the peak value of 13.2 GPa at 12 months and then declined to a value of 8.0 GPa at 24 months. Also, ultimate load peaked at 12 months with a value of 20.6 ± 0.7 N and decreased to 18.6 ± 1.4 N with no significance. These peak values were maintained through 11 months of age (Ferguson et al., 2003). Elastic stiffness reduced substantially at the age of 24 months compared to the peak elastic stiffness at 12 months (Ferguson et al., 2003).

In our study, clear differences in structural properties, e.g. ultimate load, elastic stiffness and work to failure, were observed. Specifically, femurs and tibiae showed a significant decrease in these structural properties with most of the changes observed at 22 months compared to 6 months. Ulnae also showed some significant increase in the structural properties with age.

Currey studied the mineral content of the bone and found that it increases with aging but the mineral content over the bone skeleton does not change. It increases the ultimate load and decreases the toughness of the bone (Currey, 1969). Currey also reported an inverse relationship between stiffness and ductility in the cortical bone of both mice and humans. In addition, high mineralization content resulted in a high modulus of elasticity and low work to failure and eventually low toughness (Currey, 1984). Ritchie et al. demonstrated that non-enzymatic cross-linking in the collagen increases with aging, which reduces the post yield deformation in collagen fibers thereby resulting in the reduction in toughness (Ritchie and Nalla, 2006). Gautieri et al. also reported that the increased cross-linking in the collagen fibers reduces toughness and increases the ultimate load and elastic stiffness of the bone (Gautieri et al., 2014).

The femurs and tibiae contain both cortical and trabecular bone, while ulna have minimal trabecular bone. With this in mind, these findings suggest that the loss of trabecular bone plays a more dominant role in aging. Beamer et al. reported that inbred strains including C57BL/6 mice showed no bone loss until 12 months of age (Beamer et al., 1996) and these results are in strong agreement with our work. Most of the published data is based on the studies conducted on femurs and the data presented in this paper shows similar behavior in structural properties of femurs and tibiae. On the other hand, the ulnae showed a different behavior.

Femurs showed a decline in the material properties in both males and females while tibiae showed no changes except for compressive strength, which decreased in female tibiae at 22 months of age. Male ulnae showed no changes while female ulnae showed enhanced material properties with aging (Fig. 7).

The moment of inertia decreased in male tibiae but increased in female femurs at 12 months of age only. No changes were observed in rest of the bones. Moment of inertia is a geometric property and directly dependent on the cross-sectional area of the bone. However, no changes were observed in the cross-sectional area of the bones with aging. The

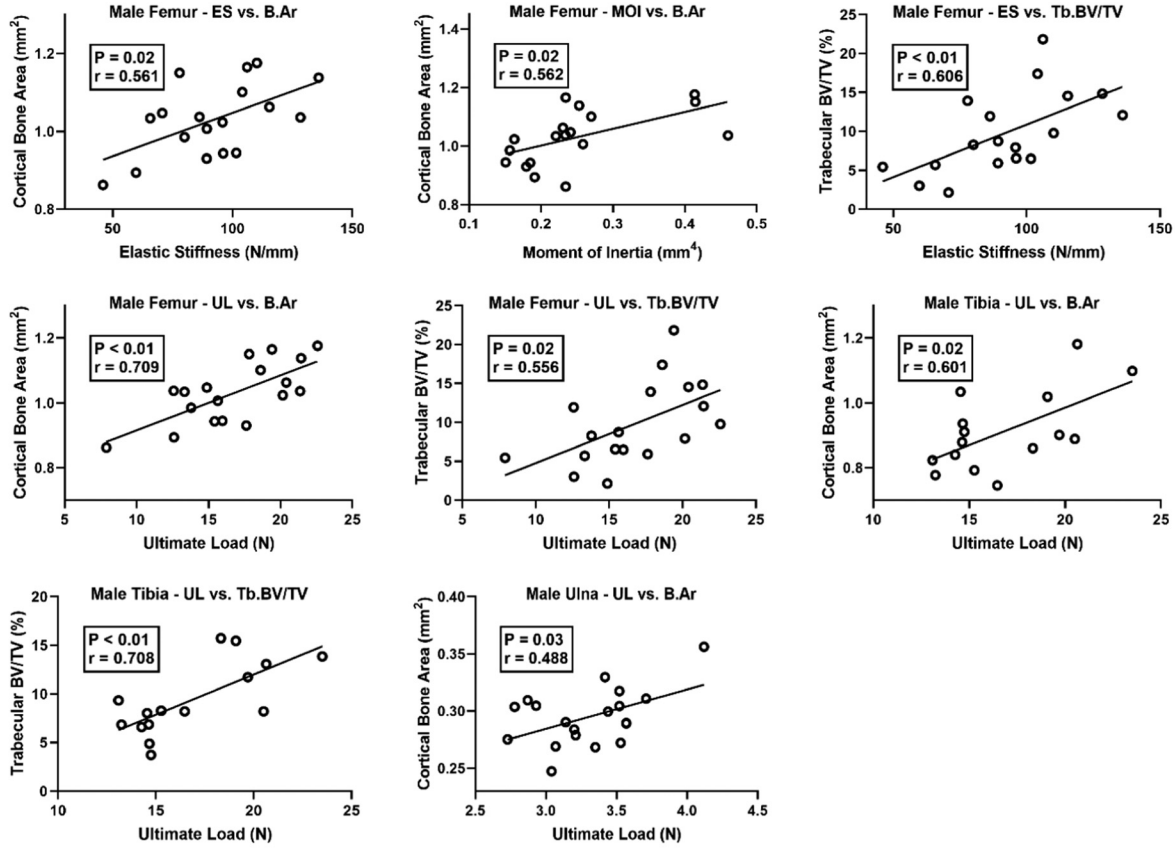

Male Femur				
	Ultimate Load	Elastic Stiffness	Modulus of Elasticity	Moment of Inertia
Cortical BV/TV				
Trabecular BV/TV				
Cortical Bone Area				
Male Tibia				
	Ultimate Load	Elastic Stiffness	Modulus of Elasticity	Moment of Inertia
Cortical BV/TV				
Trabecular BV/TV				
Cortical Bone Area				
Male Ulna				
	Ultimate Load	Elastic Stiffness	Modulus of Elasticity	Moment of Inertia
Cortical BV/TV				
Trabecular BV/TV	N/A	N/A	N/A	N/A
Cortical Bone Area				

Positive Correlation ($p < 0.05$) Negative Correlation ($p < 0.05$) Not Significant

Fig. 8. Graphs of biomechanical parameters showing significant correlation with microCT parameters (males) while *p* was set to 0.05. Pearson correlation value is shown as "r" in each graph.

diameter of the bone increases with aging but cortical thickness decreases and hence the moment of inertia showed no significant changes in most of the cases. Based on the observations and in light of previous literature, the biomechanical properties declined for both femur and tibia, but did not decline for the ulna.

Sex differences were also examined in this data. Tensile strength in ulnae, and elastic displacement along with elastic stiffness in femur were significantly different between sexes at 12 months while there were no differences found in tibiae. A considerable difference was observed at the age of 22 months in all the bones while most of the differences were found in tibiae.

To partially explain the results obtained from the biomechanical parameter analysis, microCT analysis was performed, and the biomechanical parameters were correlated with the microCT parameters. Cortical BV/TV, trabecular BV/TV and cortical bone area were calculated and correlated with ultimate load, elastic stiffness, modulus of

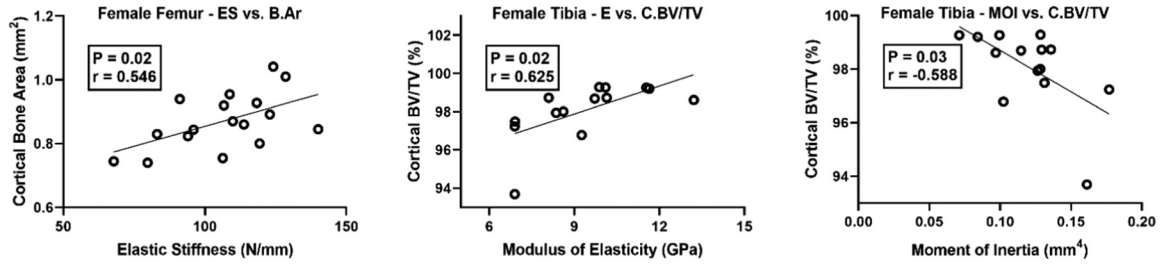

Female Femur				
	Ultimate Load	Elastic Stiffness	Modulus of Elasticity	Moment of Inertia
Cortical BV/TV				
Trabecular BV/TV				
Cortical Bone Area				
Female Tibia				
	Ultimate Load	Elastic Stiffness	Modulus of Elasticity	Moment of Inertia
Cortical BV/TV				
Trabecular BV/TV				
Cortical Bone Area				
Female Ulna				
	Ultimate Load	Elastic Stiffness	Modulus of Elasticity	Moment of Inertia
Cortical BV/TV				
Trabecular BV/TV	N/A	N/A	N/A	N/A
Cortical Bone Area				

Positive Correlation ($p < 0.05$) Negative Correlation ($p < 0.05$) Not Significant

Fig. 9. Graphs of biomechanical parameters showing significant correlation with microCT parameters (females) while *p* was set to 0.05. Pearson correlation value is shown as "r" in each graph.

elasticity and moment of inertia. The Pearson correlation analysis was done by merging all the age groups together into one group and the significance level was set to 0.05. The correlation results which were found significant for all the male bones are shown in Fig. 8 and females are shown in Fig. 9.

We observed that the cortical BV/TV did not influence any of the biomechanical parameters in all type of male bones. Ultimate load is positively correlated with the trabecular BV/TV and cortical bone area in all male bones, which suggests that the strength of the bone can be maintained with aging if these parameters does not change significantly. Elastic stiffness of the male femur is positively correlated with the trabecular BV/TV and cortical bone area too. Moment of inertia of male femur increases with the increase in the cortical bone area.

Elastic stiffness of the female femurs is positively correlated to the cortical bone area. Cortical BV/TV does not play a role in the biomechanical response (UL and ES). Cortical BV/TV is positively correlated to the modulus of elasticity and negatively correlated to the moment of inertia of the female tibiae. As the cortical bone area increases, it tends to increase the modulus of elasticity while it reduces the moment of inertia.

Collectively these data suggest that different bones change with aging in different fashions, while this study does not address the molecular basis of these changes. Future work focused on understanding the underlying collagen structure and how it might be changing could provide a means to address this question.

The biomechanical response of the skeleton starts to decline after reaching maturity. The imbalance in the bone resorption and formation results in the bone loss leading to increased risk of fracture. However, a detailed study on human skeleton is extremely difficult to accomplish and that is why there is still insufficient understanding of how human bones age. An aging study of the mouse skeleton is presented in this paper to ascertain changes in the response of different bones.

This unique study performed on three different bones of the same mice provided us an opportunity to perform direct comparisons of different bones of the same skeleton. Femur, tibia and ulna all behaved differently in terms of biomechanical parameters. Therefore, we conclude that the study of the bones should be performed in a site-specific manner and one cannot extrapolate the data of one bone to another bone or generalize it to the entire skeleton.

Most of the sex differences were found at 22 months of age, which suggests that the biomechanical response of both males and females were similar from 6 months to 12 months and showed changes only with advanced aging.

Normal aging of the mouse skeleton does closely mimic the normal aging of human skeleton. Moran et al. demonstrated that estrogen levels are maintained in mature C57BL/6 female mice (Moran et al., 2007). Recker et al. studied the perimenopausal bone loss and concluded that significant bone loss was caused by estrogen deprivation in women (Recker et al., 2000). In our study, no significant differences were observed between mature male and female mice up through 12 months of age, and this may be due to adequate levels of estrogen, which are maintained during aging in C57BL/6 mice.

An important finding from all the data is that different bones behave differently at different ages. These differences appear to be due to shape differences and biomechanical properties. Therefore, investigators using the mouse aging models should be careful to draw conclusions only on the bones being studied and not attempt to make broad generalizations to the entire skeleton.

Supplementary data to this article can be found online at https://doi.org/10.1016/j.bonr.2020.100266.

Transparency document

The Transparency document associated with this article can be found, in online version.

Credit author statement

Hammad Mumtaz: work related to experiments, analysis, discussions and conclusion and writing parts of the paper Mark Dallas: Helped with the microCT aspects of the work Mark Begonia: Worked to develop biomechanical and microCT data analysis Nuria Lara-Castillo: Helped with the animal aspects of the study JoAnna M. Scott: Performed the statistical analysis for the paper Mark L. Johnson: PI of the project 4 of the Program Project Grant that this work falls under and helped with design of the study, contribution to discussions and review of the paper Thiagarajan Ganesh: Overall management of the study including writing the work in paper form, identifying the biomechanical parameters required for the analysis, data analysis and development of the revised version responses.

Acknowledgements

This work was funded by a grant from the National Science Foundation award number NSF-CMMI- 1662284 (PI: Thiagarajan Ganesh) and National Institutes of Health – NIA P01 AG039355 (LF Bonewald-PI) & NIAMS R01 AG053949 (ML Johnson – PI).

References

Beamer, W., Donahue, L., Rosen, C., Baylink, D., 1996. Genetic variability in adult bone density among inbred strains of mice. Bone 18, 397–403.
Begun, D.L., 2015. Age-Related Changes in Bone: Variation and Factors Influencing Bone Fragility.
Boskey, A.L., Coleman, R., 2010. Aging and bone. J. Dent. Res. 89, 1333–1348.
Boskey, A.L., Imbert, L., 2017. Bone quality changes associated with aging and disease: a review. Ann. N. Y. Acad. Sci. 1410, 93.
Brodt, M.D., Ellis, C.B., Silva, M.J., 1999. Growing C57BL/6 mice increase whole bone mechanical properties by increasing geometric and material properties. J. Bone Miner. Res. 14, 2159–2166.
Currey, J.D., 1969. The relationship between the stiffness and the mineral content of bone. J. Biomech. 2, 477–480.
Currey, J.D., 1984. Effects of differences in mineralization on the mechanical properties of bone. Philosophical Transactions of the Royal Society of London. B, Biological Sciences 304, 509–518.
Ensrud, K.E., Palermo, L., Black, D.M., Cauley, J., Jergas, M., Orwoll, E.S., Nevitt, M.C., Fox, K.M., Cummings, S.R., 1995. Hip and calcaneal bone loss increase with advancing age: longitudinal results from the study of osteoporotic fractures. J. Bone Miner. Res. 10, 1778–1787.
Ferguson, V.L., Ayers, R.A., Bateman, T.A., Simske, S.J., 2003. Bone development and age-related bone loss in male C57BL/6J mice. Bone 33, 387–398.
Gautieri, A., Redaelli, A., Buehler, M.J., Vesentini, S., 2014. Age-and diabetes-related nonenzymatic crosslinks in collagen fibrils: candidate amino acids involved in advanced glycation end-products. Matrix Biol. 34, 89–95.
Glatt, V., Canalis, E., Stadmeyer, L., Bouxsein, M.L., 2007. Age-related changes in trabecular architecture differ in female and male C57BL/6J mice. J. Bone Miner. Res. 22, 1197–1207.
Glynn, W.N., Meilahn, E.N., Charron, M., Anderson, S.J., Kuller, L.H., Cauley, J.A., 1995. Determinants of bone mineral density in older men. J. Bone Miner. Res. 10, 1769–1777.
Harvey, N., Dennison, E., Cooper, C., 2010. Osteoporosis: impact on health and economics. Nat. Rev. Rheumatol. 6, 99.
Heveran, C.M., Schurman, C.A., Acevedo, C., Livingston, E.W., Howe, D., Schaible, E.G., Hunt, H.B., Rauff, A., Donnelly, E., Carpenter, R.D., 2019. Chronic kidney disease and aging differentially diminish bone material and microarchitecture in C57Bl/6 mice. Bone 127, 91–103.
Jämsä, T., Jalovaara, P., Peng, Z., Väänänen, H.K., Tuukkanen, J., 1998. Comparison of three-point bending test and peripheral quantitative computed tomography analysis in the evaluation of the strength of mouse femur and tibia. Bone 23, 155–161.
Jepsen, K.J., 2009. Systems analysis of bone. Wiley Interdiscip. Rev. Syst. Biol. Med. 1, 73–88.
Jilka, R.L., 2013. The relevance of mouse models for investigating age-related bone loss in humans. Journals of Gerontology Series A: Biomedical Sciences and Medical Sciences 68, 1209–1217.
Lara-Castillo, N., Kim-Weroha, N.A., Kamel, M.A., Javaheri, B., Ellies, D.L., Krumlauf, R.E., Thiagarajan, G., Johnson, M.L., 2015. In vivo mechanical loading rapidly activates beta-catenin signaling in osteocytes through a prostaglandin mediated mechanism. Bone 76, 58–66.
Melton III, L.J., 1997. The prevalence of osteoporosis. J. Bone Miner. Res. 12, 1769–1771.
Mesner, L.D., Calabrese, G.M., Al-Barghouthi, B., Gatti, D.M., Sundberg, J.P., Churchill, G.A., Godfrey, D.A., Ackert-Bicknell, C.L., Farber, C.R., 2019. Mouse genome-wide association and systems genetics identifies Lhfp as a regulator of bone mass. PLoS Genet. 15, e1008123.
Moran, A.L., Nelson, S.A., Landisch, R.M., Warren, G.L., Lowe, D.A., 2007. Estradiol replacement reverses ovariectomy-induced muscle contractile and myosin dysfunction in mature female mice. J. Appl. Physiol. 102, 1387–1393.
Recker, R., Lappe, J., Davies, K., Heaney, R., 2000. Characterization of perimenopausal bone loss: a prospective study. J. Bone Miner. Res. 15, 1965–1973.
Ritchie, R., Nalla, R., 2006. Fracture, aging and disease in bone and teeth. In: Fracture of Nano and Engineering Materials and Structures. Springer, pp. 23–24.
Schriefer, J.L., Robling, A.G., Warden, S.J., Fournier, A.J., Mason, J.J., Turner, C.H., 2005. A comparison of mechanical properties derived from multiple skeletal sites in mice. J. Biomech. 38, 467–475.
Somerville, J., Aspden, R.M., Armour, K., Armour, K., Reid, D.M., 2004. Growth of C57BL/6 mice and the material and mechanical properties of cortical bone from the tibia. Calcif. Tissue Int. 74, 469–475.
Syed, F.A., Hoey, K.A., 2010. Integrative physiology of the aging bone: insights from animal and cellular models. Ann. N. Y. Acad. Sci. 1211, 95–106.
Vennin, S., Desyatova, A., Turner, J.A., Watson, P., Lappe, J.M., Recker, R.R., Akhter, M.P., 2017. Intrinsic material property differences in bone tissue from patients suffering low-trauma osteoporotic fractures, compared to matched non-fracturing women. Bone 97, 233–242.